University of Windsor

Mechanical, Automotive, & Materials Engineering
401 Sunset Avenue
Windsor, Ontario, Canada N9B 3P4
519 253 3000 (2616)
www.uwindsor.ca/mame

Report 2: Vehicle Handling Simulation

Arjun Posarajah
104980541
MECH-4463
Vehicle Dynamics

March 14, 2022

Contents

List of Figures

Introduction

Figure A1: 1996 Honda Civic CX Hatchback [3] Markus

The car chosen for the handling dynamics analysis is a 1996 6th generation Honda Civic CX hatchback. The car is a five-speed manual car with a 4-stroke spark ignition engine and a forward wheel drive configuration. Interest to choose this car stems from that this was family car when growing up so with a prior experience of the vehicle giving me better insight and for the fact that the Honda Civic is a very common car allowing for vast amount of data to be used. The overall purpose is to perform a thorough analysis of the longitudinal dynamic capability of the 1996 6th generation Honda Civic CX hatchback.

1 Vehicle Behaviour

1.1 Calculation for Vehicle Behaviour

The assumption of cf and cr at 80000Nm/s for all calculations as acquiring information for this vehicle was not possible.

$$u_{char} = \sqrt{\frac{(a+b)^2(c_f)(c_r)}{m(bc_r - ac_f)}}$$

$$u_{char} = \sqrt{\frac{(3.172)^2(80000)(80000)}{1008((2.0058(80000) - (1.172)(80000))}}$$

$$u_{char} = 30.932\frac{m}{s} = 111.36\ km/hr$$

Figure 1.1: Calculations for characteristic speed.

$$d_0 = \frac{(a+b)^2 c_f c_r}{mI_{zz}u^2} + \frac{ac_f - bc_r}{I_{zz}}$$

$$d_0 = \frac{(3.172)^2(80000^2)}{1008(1785)(30.932)^2} + \frac{1.1712(80000) - 2.0058(80000)}{1785}$$

$$d_0 = 74.885$$

Figure 1.2: Calculation for d0.

$$d_1 = \frac{a^2 c_f + b^2 c_r}{I_{zz} u} + \frac{c_f + c_r}{mu}$$

$$d_1 = \frac{(1.172)^2(80000) + (2.0058)^2(80000)}{(1785)(30.932)} + \frac{2(80000)}{(1008)(30.932)}$$

$$d_1 = 12.962$$

Figure 1.3: Calculation for d1.

$$s = -\frac{d_1}{2} \pm \sqrt{\left(\frac{d_1}{2}\right)^2 - d_0}$$

$$s = -\frac{12.962}{2} \pm \sqrt{\left(\frac{12.962}{2}\right)^2 - 74.885}$$

$$s = -6.481 \pm 5.734i$$

Figure 1.4: Calculation for s.

$$\omega_n = \sqrt{(-6.481)^2 + (5.734)^2}$$

$$\omega_n = 8.653 \frac{rad}{s} = 1.377hz$$

Figure 1.5: Calculation for natural frequency.

$$\xi = \frac{6.481}{8.653} = 0.749$$

$$\tau = \frac{1}{\xi(\omega_n)} = \frac{1}{(0.749)(8.653)} = 0.154$$

Figure 1.6: Damping ratio and τ calculation.

$$(u_{transient})^2 = \frac{I_{zz}}{4(bc_r - ac_f)}\left(\frac{a^2 c_f + b^2 c_r}{I_{zz}} + \frac{c_f + c_r}{m}\right)^2 - u_{char}^2$$

$$(u_{transient})^2 = \left(\frac{1785}{4(80000)(2.0058 - 1.1712)}\right)\left(\frac{80000(1.172^2 + 2.0058^2)}{1785} + \frac{80000(2)}{1008}\right)^2 - (30.932^2)$$

$$u_{transient} = 9.5\frac{m}{s} = 34.2\frac{km}{hr}$$

Figure 1.7: Calculation for transient speed.

1.2 Analysis of Vehicle Behaviour

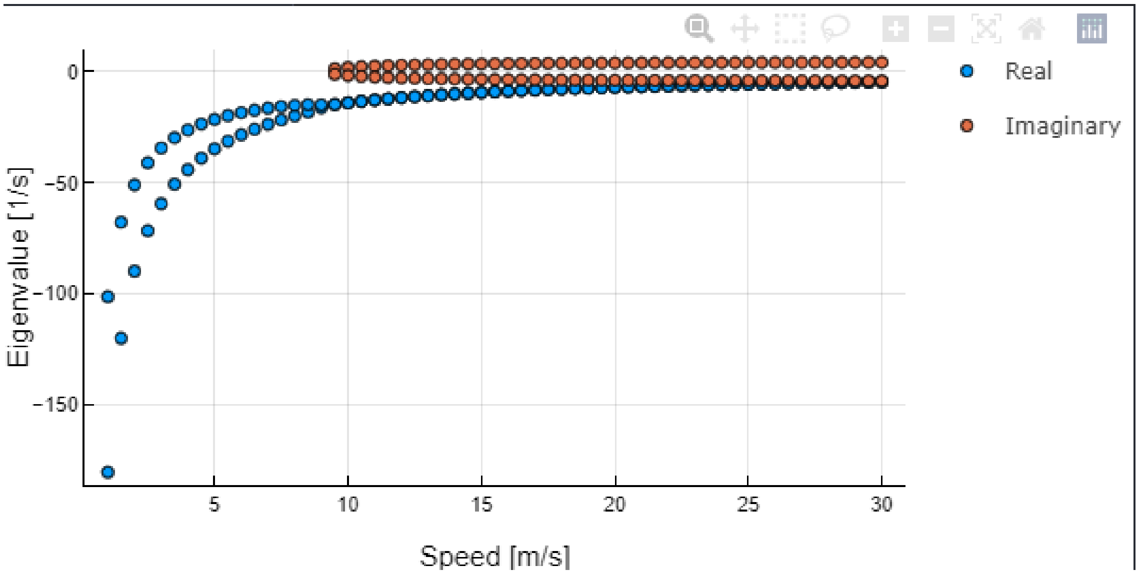

Figure 1.8: Eigenvalue vs speed graph.

The vehicle behaviour is experiencing understeer. This is seen from figure 1.8, as the appearance of imaginary component from the Eigenvalue graph it is a clear indication of understeer. With the eigenvalues of the equation of motion are complex with negative real parts shows a stable but oscillatory system. The real part indicates decreasing yaw damping as speed increases. The speed where the transient response of the vehicle shifts from pure decay to an oscillatory decay is at 9.5m/s which was found through figure 1.7. When comparing that value with the graph in figure 1.8, as the speed had increased the real roots for indicate a tendency for the oscillatory behaviour. The negative real parts indicate the amplitude of the oscillation had decreased with the time and remained stable at all speeds. Due to the effective damping decreases while increasing the speed, the motion will take longer in high-speed situations. Imaginary numbers start to appear where transient speed occurs which confirms this. This is a feasible range as this is to happen at low speeds and 9.5m/s is as such.

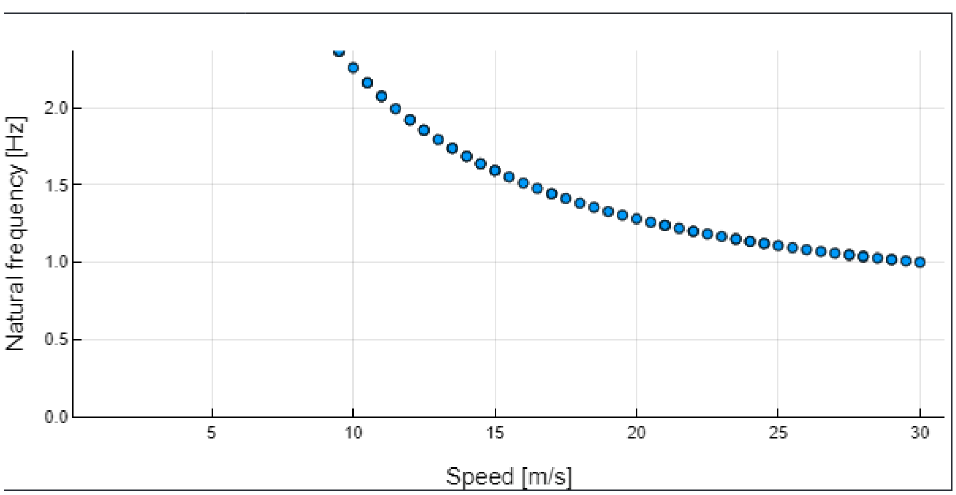

Figure 1.9: Natural frequency vs. Speed Graph.

The natural frequency is at 1.377hz which is not at the top or bottom in figure 1.9 graph showing it is not near the end showing it is able to be excited by steering or external forces. With the trend in figure 1.9, the natural frequency is starting to become normalized at around 1hz, which therefore proving that at 1.377hz it is still open to be excited by steering or external forces. With the speed increasing the frequency decreases leading to more stability in terms of understeer cars. When considering if there is enough sufficient damping to prevent excessive yaw motion the relationship between natural frequency and damping ratio is used. The frequency response of the yaw when in understeer shows a slight resonance effect around the natural frequency but this is only at high speeds does the yaw damping decrease. The damping ratio being divided by natural frequency directly correlates the influence at which at lower speeds with a high natural frequency would in turn give a better damping ratio leading to prevent more yaw motion. However, with the increase in speed the damping ratio decreases as well seen in figure 1.10, ultimately creating more yaw motion. When the speed gets high enough the peak is seen in figure 1.11 is more apparent with the resonant frequency.

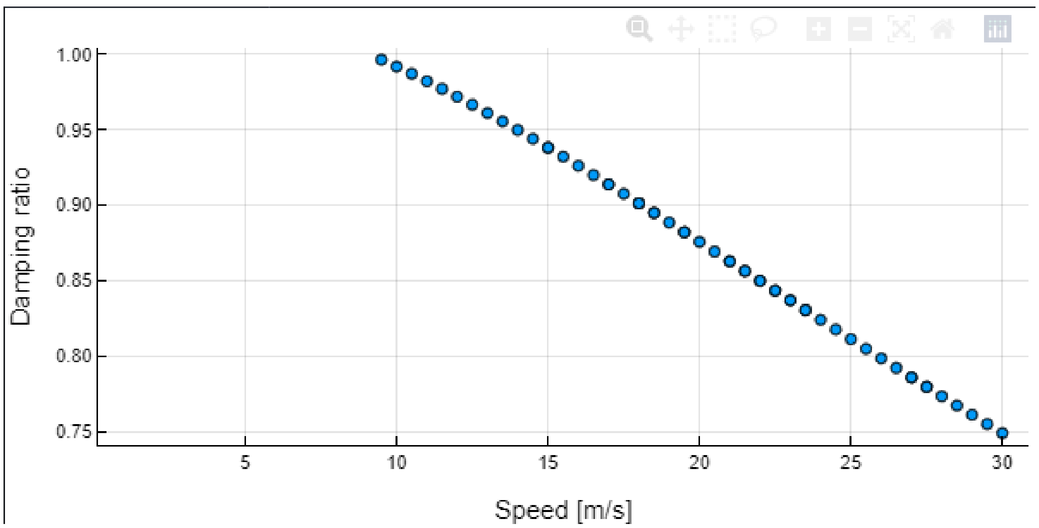

Figure 1.10: Damping ratio vs. Speed Graph.

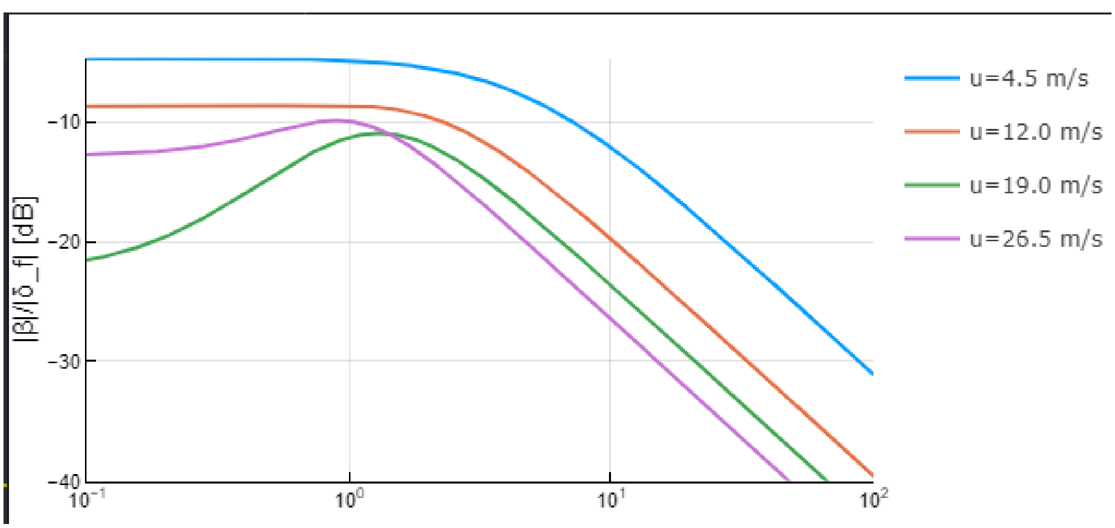

Figure 1.11: Body slip angle vs frequency Graph.

1.3 Yaw Rate Sensitivity

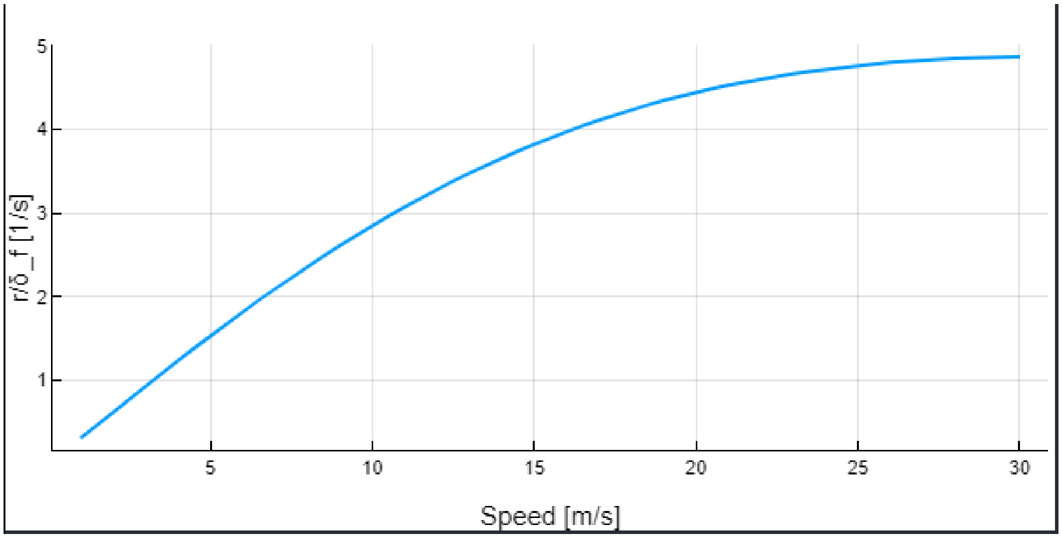

Figure 1.12: Yaw rate sensitivity vs speed graph.

Considering the steady state response data, from figure 1.1, the characteristic speed of 30.932m/s. In figure 1.12, it is evidently seen from the graph that at characteristic speed, the maximum yaw rate sensitivity is 4.873 s^{-1}. When considering all the relationships at characteristic speed, it is the maximum yaw rate sensitivity because it is where the frequency and damping ratio are at the lowest. With an increase in sensitivity with the increasing of speed reaching a maximum ultimately at the characteristic speed since the car is understeer further having no resonance with it not being an underdamped system, otherwise would have to consider critical speed. With the slight resonance around the natural frequency and when the speed increases to reduce the yaw damping.

2 Steering Input

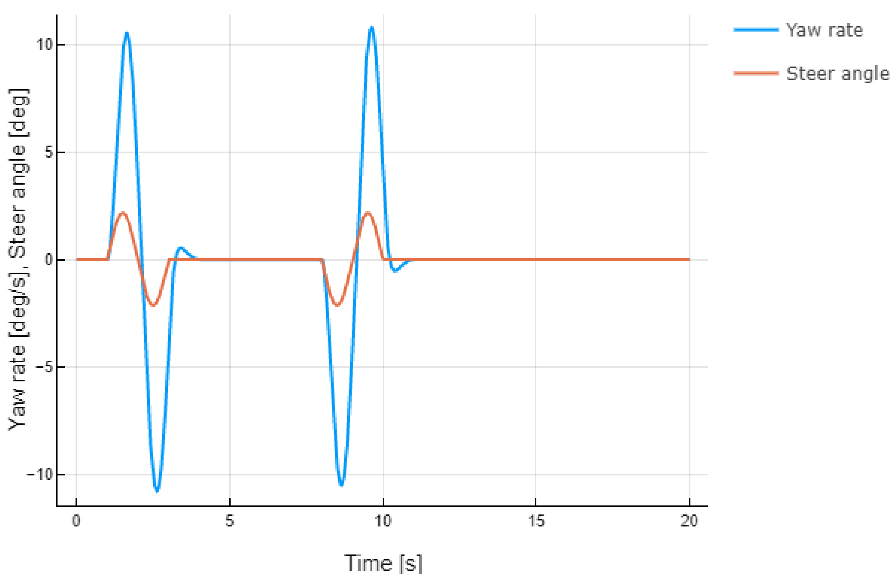

Figure 2.1: Yaw rate r vs time graph.

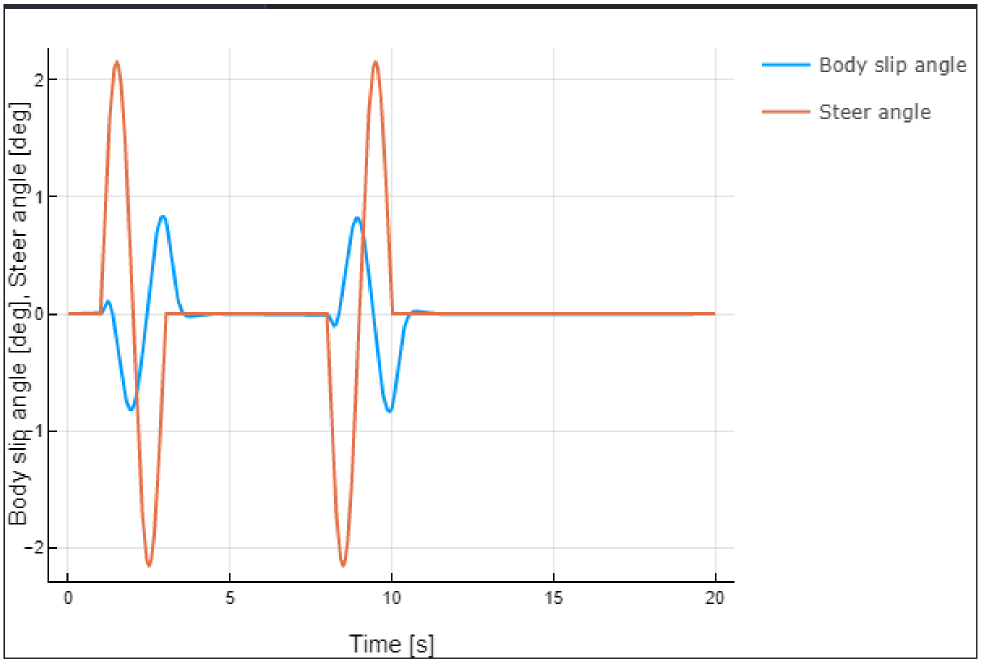

Figure 2.2: Body slip vs Time Graph.

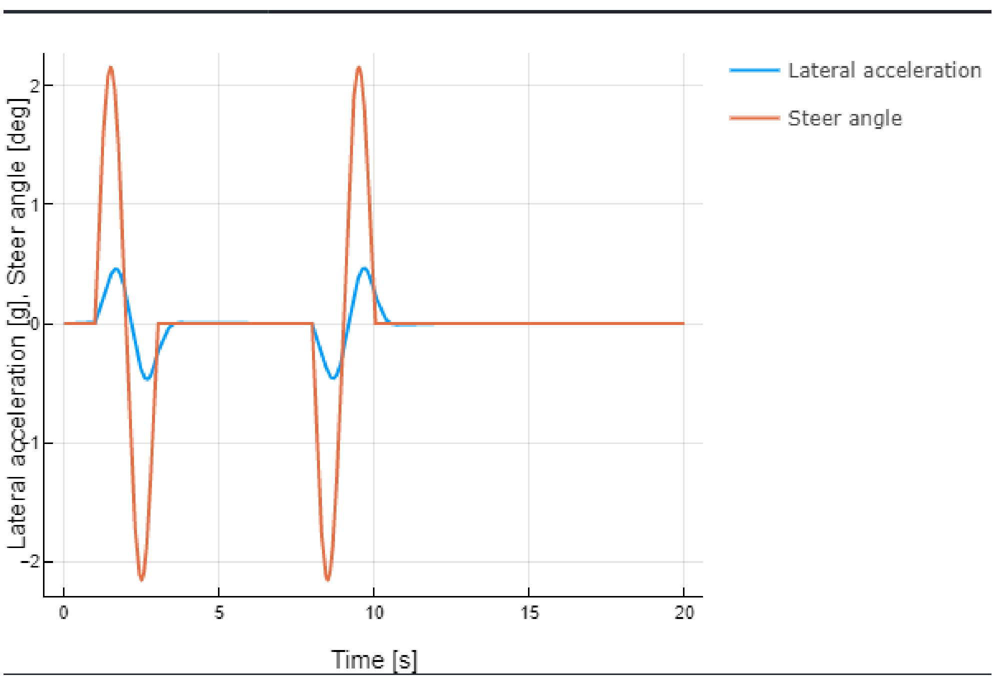

Figure 2.3: Lateral Acceleration vs Time graph.

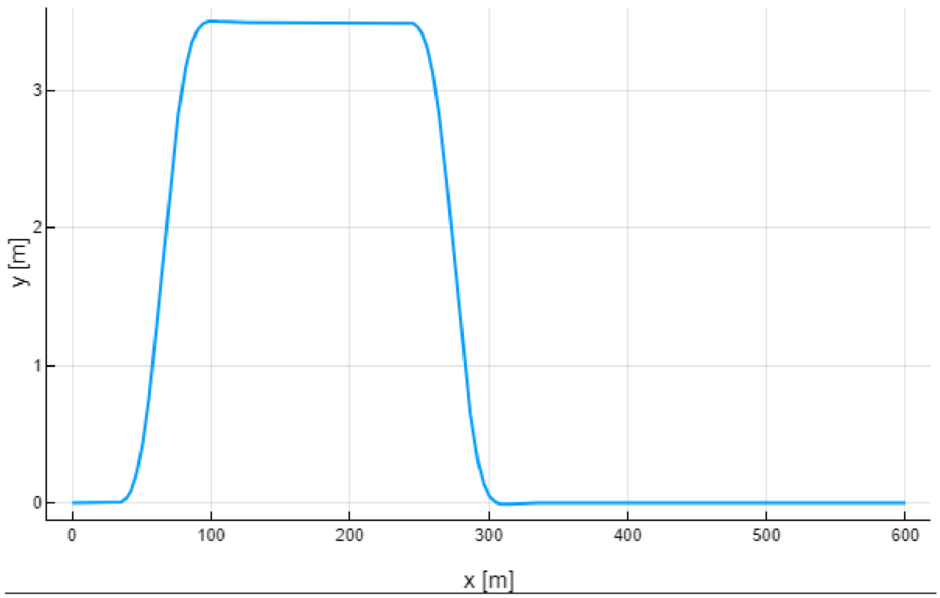

Figure 2.4: Path of the vehicle.

The physical significance of the results shows the at the first second to the third second the vehicle takes a left turn and holds for 5 seconds then returns within 2 seconds in figure 2.4. This is further analysed in figure 2.1, where when the car takes the turn, the steer angle turns the yaw rate increases positively until the steer angle is at zero then yaw rate becomes negative when the steer angle tries to level out and ultimately creates an extra positive bump of yaw rate after steer angle levels at 0. This is the force of the vehicle pushing out due to the inertial yaw force.

At the peaks of the steer angle, there is also a peak yaw rate which follows the characteristics of a steady state gain expression whereas the weight distribution and speed of the vehicle are the main factors. As seen, these will be under influence especially when considering cornering in this situation where the weight distribution will move laterally as seen in figure 2.3 where the acceleration occurs at an offset to the steer angle showing the vehicle is reacting to the weight distribution to the turn that was being simulated.

The simulation is fairly accurate prediction to how the vehicle will act in this situation, which was for the first answer of it did make sense. When analysing the figures above, in figure 2.1, as the car turns to the left the angle of yaw is also to the left at a higher rate due to the impact of weight distribution and damping capability. When viewing figure 2.2, the steer angle is inversely and offset at the peaks of the steer angle and body slip angle. This is due to the car trying to recorrect itself through understeer and the weight distribution creating kick out force causing the body slip to occur. When analysing figure 2.3, the occurs to have high lateral acceleration at peaks of steer angle showing when the car decides to change direction the rest of the car has to pull along as well regardless of original direction causing high lateral acceleration to be able to pull the car to the desired direction.

Error could occur because of the steer angles occurring at robotic sharp angles which is impractical. When considering the most drivers do not sharply turn their steering wheels when making turns it would affect the simulations. The steering angle would smoothly go through the sine process, this sharp angle turn could also incur jerk motion to the car leading to not reliable information. Assuming constant speeds is another error, as most driver either accelerate or decelerate when taking a turn, with a more realistic outcome instead with the simulation a constant velocity is set. This leads to the car taking the turn with no acceleration causing an error of unrealistic simulation occurring to analyze.

The transient behaviour of the slip angle immediately after the steer not peaking at the same time and is offset as this is due to weight transfer. This is seen in figure 2.2, the peaks are inversely correlated and offset, this is unexpected behaviour as all other peaks were together. As this vehicle corners, the transient phase occurs where the body slip angle fluctuates to a steady state phase but oversteer and understeer act similarly in low speeds where the rear axle tracks inside the front for both configurations. Which what was unexpected as it would have been a oversteer configuration with the same results. As both understeer and oversteer will transition to a tail out condition with speed increase but it slightly different for oversteer. So, as understeer car the transient behaviour is the tail out condition which occurs after the steer angle begins to change, where the rear axle tracks the inside of the front which is unexpected as both configurations act the same in low speeds which is exactly the scenario which was simulated.

3 Adjusted Locations Simulations

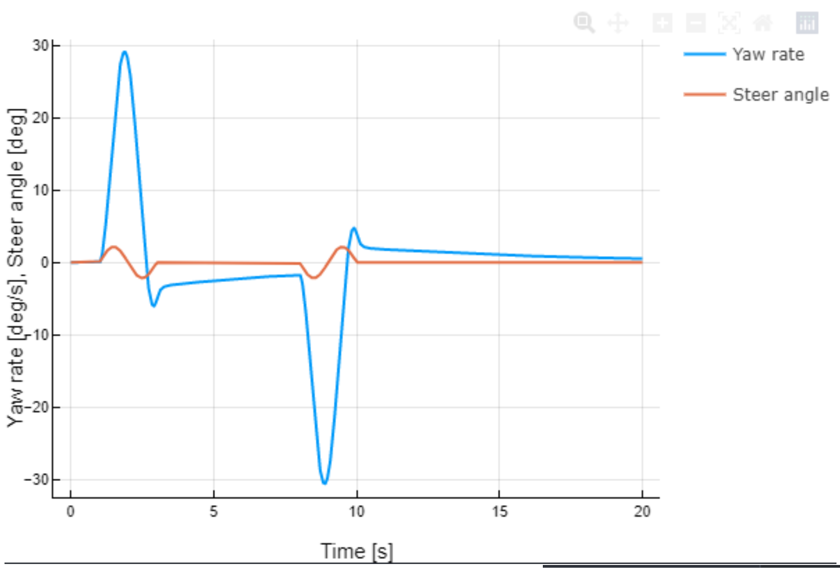

Figure 3.1: Yaw rate vs time graph.

Figure 3.2: Body slip vs Time Graph.

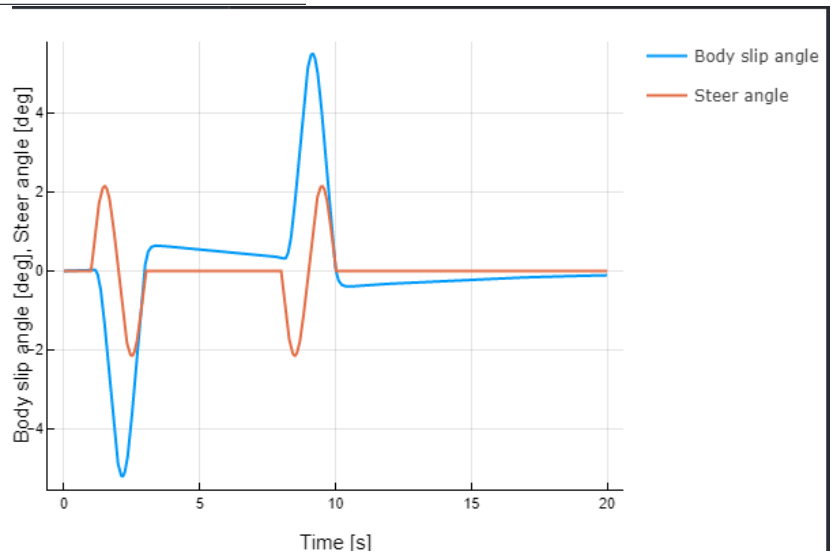

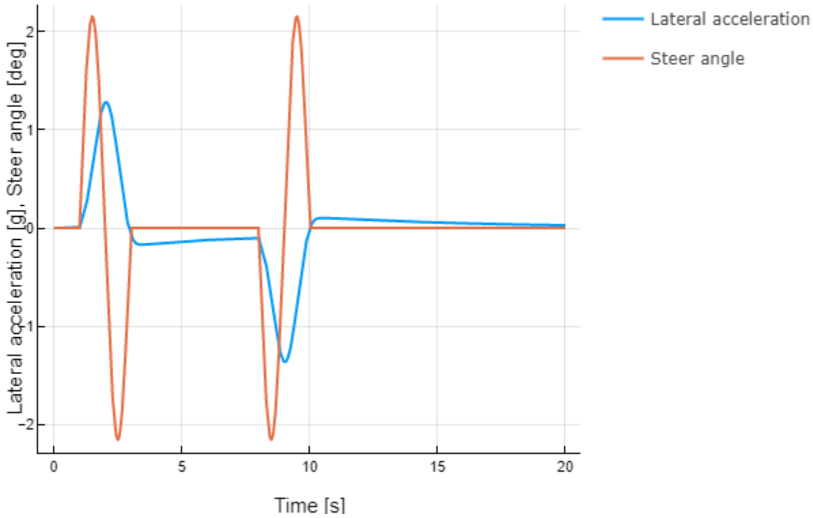

Figure 3.3: Lateral Acceleration vs Time Graph.

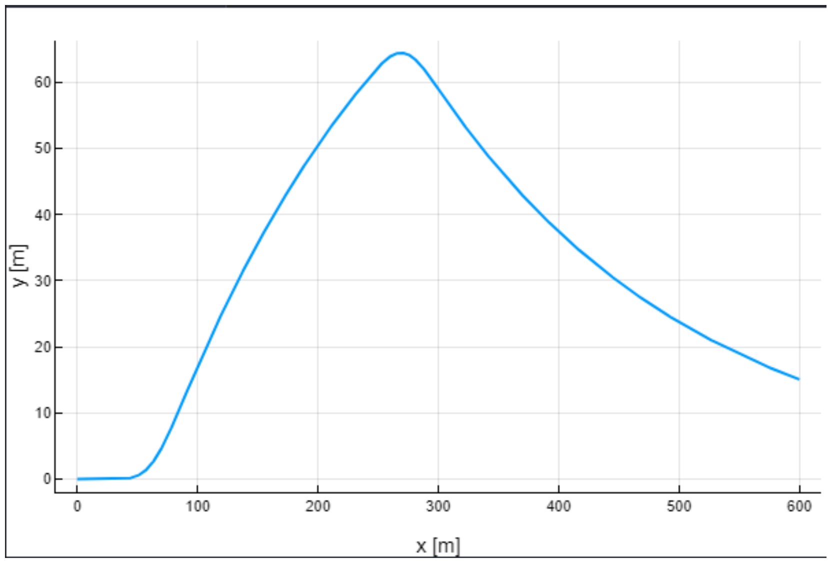

Figure 3.4: Path of the Vehicle.

Under the same circumstances and Julia code as section 2, when adjusting the centre of mass of the vehicle to become a oversteer configuration, the car simply does not do the same path as the understeer configuration as seen in figure 3.4.

When analyzing figure 3.1, as the first steer angle change occurs the yaw rate is significantly higher than on a understeer configuration and unlike understeer, the entirety of the steer angle sine on the graph is the first peak of the yaw rate and it normalizes after the steer angle is completely zero. The yaw rate after the steer angle is zero is not as high as the initial yaw rate peak, showing that as the first steer angle occurs the total force of the vehicle is shifted significantly more compared to before, yet normalises much slower with a small negative yaw rate. When viewing figure 3.2, the unusual finding is that the body slip doesn't normalize even when the steer angle is at zero which is very odd as this means regardless of if the steer wheel was leveled the car is still drifting motion. Which is slightly expected, however even at low speeds this is unusual with oversteer cars being notorious for being able to drift easier compared to understeer. When making a left turn the vehicle is experiencing the opposite body slip angle which it was like what was explained in understeer configuration however the vehicle does not have a body slip that changes signs. This means it either stays negative or positive meaning the car does not readjust but body slips one way and has body slip in the opposite way without staying at zero. Meaning the car is not stable when taking turns and will always be at a body slip angle regardless of if the steering input is corrected. When understanding figure 3.3, the car is similarly explained in figure 3.2, as both share the fact that the car does not normalize to zero after the turn is finished. This is due to the oversteering configuration and how with the car being back biased, the car is having a drift motion occurring which is happening even in the five second delay before having to come back to the initial position. The car sways with the lateral acceleration, as the car moves left so does the lateral acceleration and does not normalise depicting the drift effect.

This is what was expected as the consensus that oversteer vehicle are not as stable in terms of handling compared to understeer, which is why most commercial vehicles are understeer. However, the expectation was that it would be slightly uncontrolled, but with the exact same steering input the car becomes very unsafe to drive in comparison with the vehicle not being able to drive the same path as the understeer configuration.

4 Truck and Trailer

When running the truck simulation, the 2021 F-150 Raptor was used and assumption of parameters of the trailer dimensioning and properties.

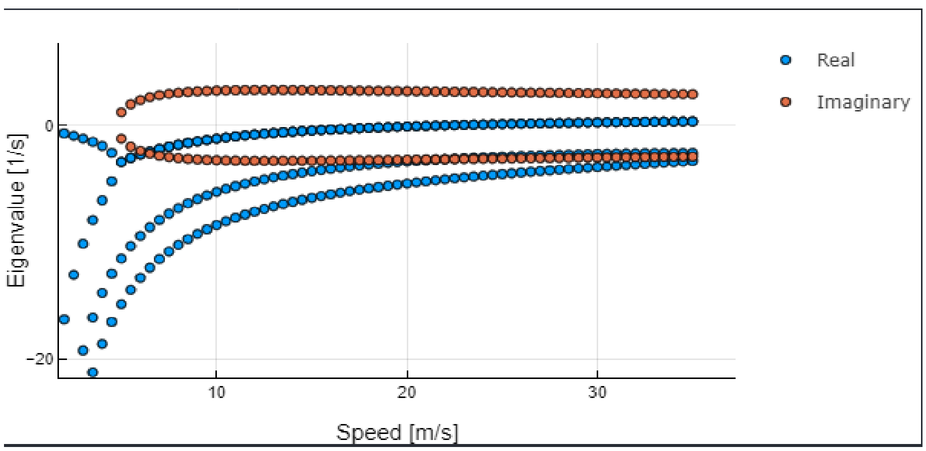

Figure 4.1: The Eigenvalue graph zoomed in to see the trends

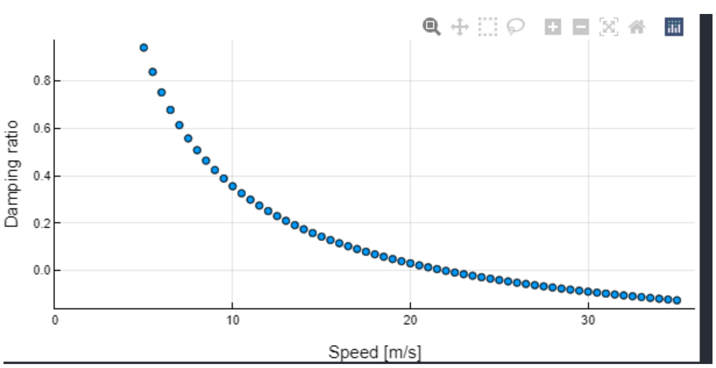

Figure 4.2: Damping ratio vs Speed

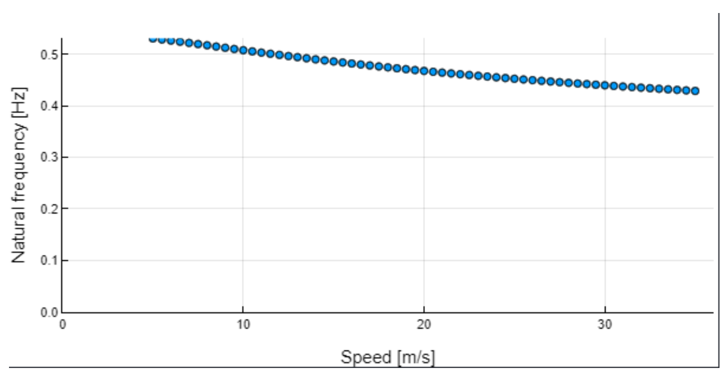

Figure 4.3:Natural Frequency vs Speed

After analyzing the vehicle and trailer, with the centre of mass of the trailer already very rearward, as this is an indication of fish tailing that would develop. As seen in the eigenvalue chart in figure 4.1, with only one real trend leveling at zero, compared to when a jack-knifing trend where two lines of real would intersect and level toward zero. With the trailers oscillations have a constant frequency and therefore creates damping in the sway to decrease with the speed which would ultimately mean it becomes unstable above the critical speed. The fish tailing with the sway is normally at 0.6Hz which is seen in figure 4.3, that it starts at 0.6Hz and slowly decrease with the speed of the vehicle. This is further proven through the damping ratio graph on figure 4.2 showing the drastic drop when increasing the speed of the vehicle leading for more oscillatory actions to occur. This ultimately proving that the vehicle will be experiencing fish tailing.

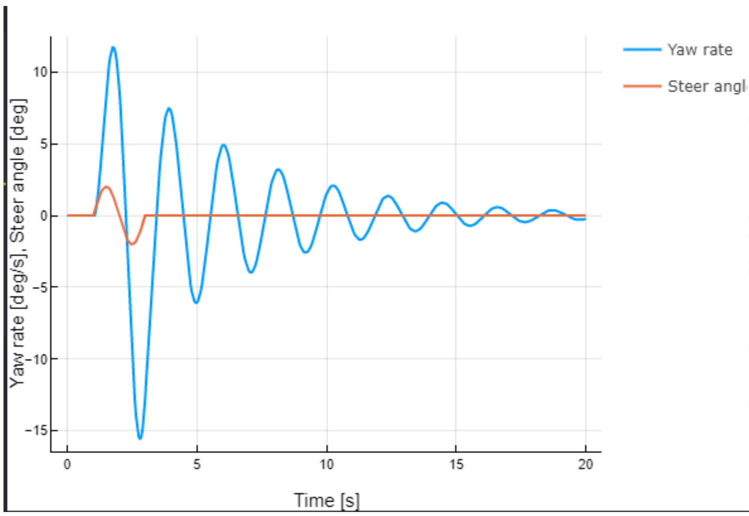

Figure 4.4: Yaw rate vs Time

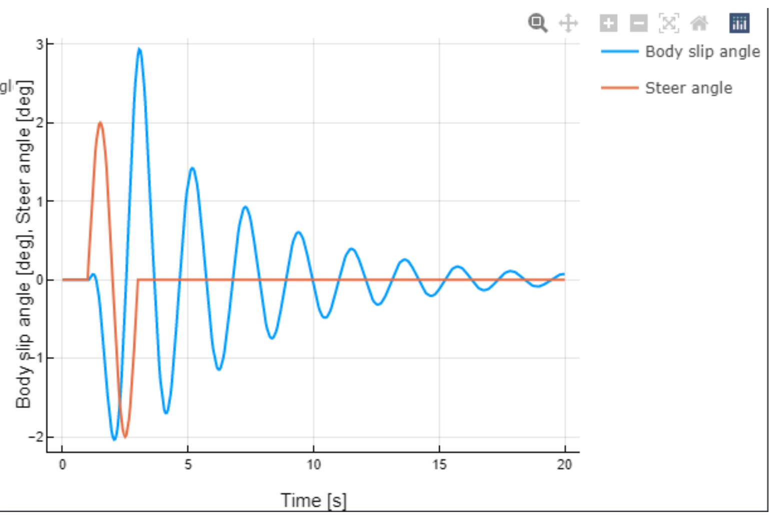

Figure 4.5 Body Slip vs Time

When analyzing the handling of the vehicle as it is fishtailing it is evidently seen in figure 4.4 and 4.5. In figure 4.4, as the steering is completed, the vehicle is still experiencing an oscillation of the yaw rate decaying. This is due to the side-to-side fish tailing motion that is occurring and showing that with the centre of mass further back on the trailer creates this oscillation affect on all vehicles and is ultimately very hard to predict.

When viewing figure 4.5, the when the vehicle take the first turn and readjusts the body slip is higher on the readjust due to a trailer in general but oscillates because of the further back centre of mass. This is interesting comparing without the vehicle in figure 2.2 where the vehicle would level and catch itself with the body slip while with the trailer it is continuously moving and fish tailing.

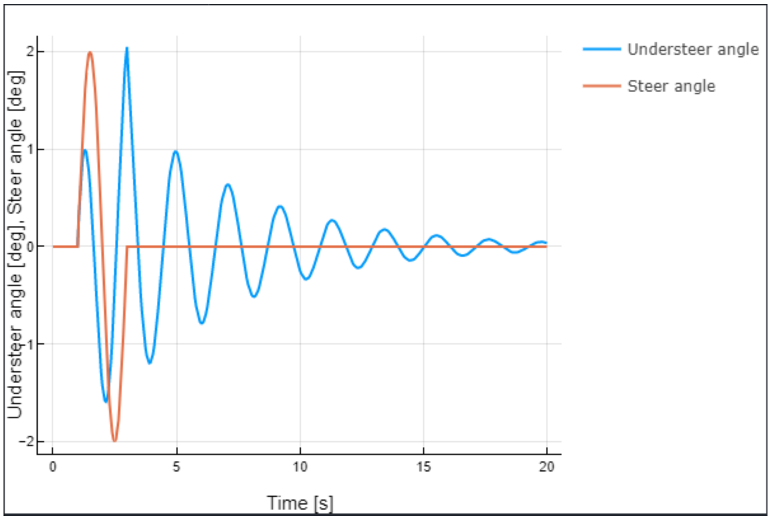

Figure 4.6: Understeer angle vs Time

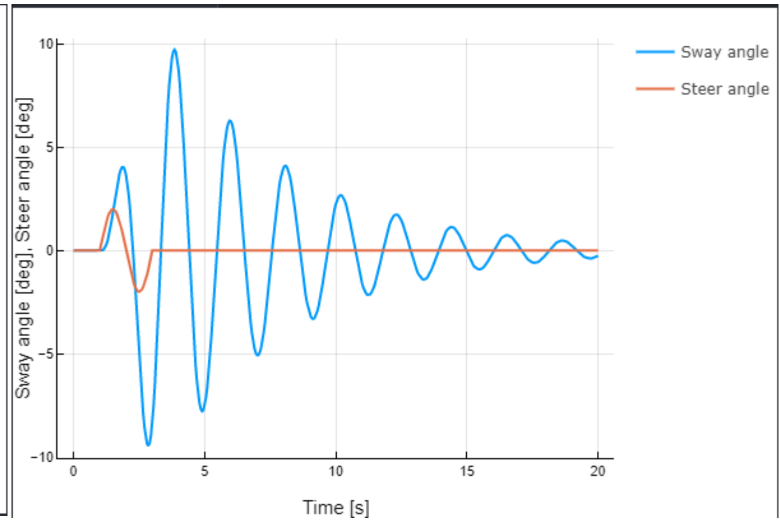

Figure 4.7: Sway angle vs Time

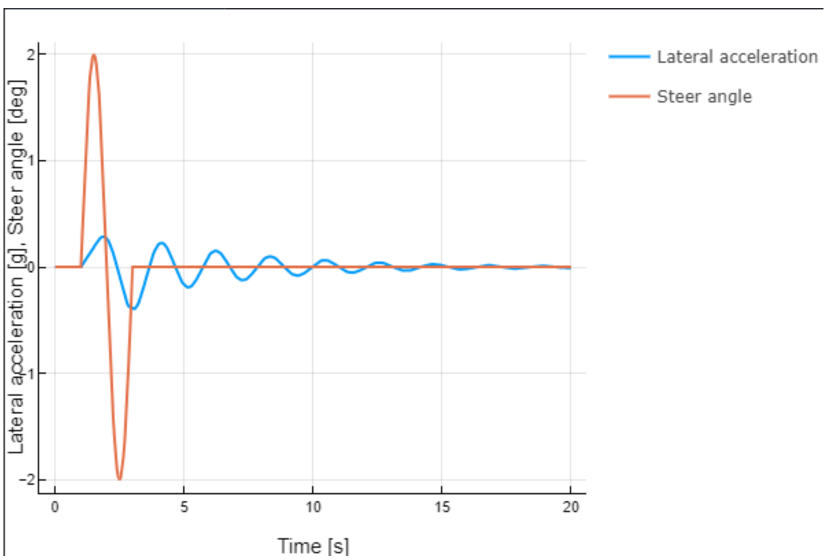

Figure 4.8: Lateral Acceleration vs Time Graph

When reviewing figure 4.6, with the understeer angle the car is going shorter than the intended steering angle, however after the second peak on the steering angle it matches the initial peak of the steering angle showing how wild and far the car is moving because of the added trailer oscillation. With the sway angle in figure 4.7, it is just further proof of the fish tailing as explained above with the lateral angle moving side to side. In figure 4.8, the lateral acceleration is small in comparison to the steer angle, yet an oscillation effect does occur during the fish tailing action.

Some conclusions on trailer safety are that the centre of mass of the trailer should be towards the hitch of the trailer, which can be done through the manufacturer of the trailer or when loading up the trailer and make sure most of the weight is at the hitch side of the trailer. Jack knifing is much more dangerous as the car would for fold up and cause a crash. With the centre of mass being closer to the hitch it would significantly lower the oscillating affects of the trailer on the vehicle creating a safer driving experience.

Conclusion

Through the researching of handling dynamics, it is evident with the understeer vehicle cornering is safer and more predictable as the yaw is more manageable but with oversteer would create a more body roll, yaw and unpredictable result as seen from section 4. With the general findings that when the oscillation had decreased with the time and remained stable at all speeds. Due to the effective damping decreases while increasing the speed, the motion will take longer in high-speed situations. Increase in speed the damping ratio decreases as well seen in figure 1.9, ultimately creating more yaw motion. This was further proven through the simulation of the turn and solidified all claims.

For trailer handling dynamics with the centre of mass of the trailer being closer to the hitch it negates and reduces the fish tailing, but as the centre of mass goes further it creates fish tailing and later jack knifing.

References

[1] “Catalog the Catalog of Cars, Car Specs Database.” *Automobile*, https://www.automobile-catalog.com/.

[2] “Honda Manual Transmission Specifications & Gear Ratios - Fuel Economy, Hypermiling, EcoModding News and Forum.” *EcoModder Wordmark*, https://ecomodder.com/forum/showthread.php/honda-manual-transmission-specifications-gear-ratios-26279.html.

[3] Markus, Frank. “Tested: 1996 Honda Civic DX Is Clean and Quick.” *Car and Driver*, Car and Driver, 29 Nov. 2021, https://www.caranddriver.com/reviews/a36521729/1996-honda-civic-dx-by-the-numbers/.

[4] “2021 Ford F-Series F-150 XIV SuperCrew Raptor 3.5 EcoBoost V6 (450 HP) 4x4 Automatic.” *Technical Specs, Data, Fuel Consumption, Dimensions,* https://www.auto-data.net/en/ford-f-series-f-150-xiv-supercrew-raptor-3.5-ecoboost-v6-450hp-4x4-automatic-43110.

[5] Minaker, Bruce P. *Fundamentals of Vehicle Dynamics and Modelling: A Textbook for Engineers with Illustrations and Examples*. Wiley, 2020.